This article has been accepted for publication in a future proceedings of this conference, but has not been fully edited. Content may change prior to final publication.
Citation information: DOI: 10.1109/VTC2025-Fall65116.2025.11310395, 2025 IEEE 102nd Vehicular Technology Conference (VTC2025-Fall)

# Artificial Noise Aided UAV-ISAC System Against Malicious Radar Signal Detection and Communication Eavesdropping

Yi Zhou*†, Xinyu Liu*, Pingzhi Fan*, Zheng Ma*, Kezhi Wang†, Zhicheng Dong‡, and Erdal Panayirci§

* Information Coding & Transmission (ICT) Key Laboratory of Sichuan Province,
Southwest Jiaotong University, Chengdu, 611756, China
† School of Computer Science, Brunel University London, London, UB8 3PH, UK
‡ School of Information Science and Technology, Tibet University, Lhasa 850011, China.
§ Department of Electrical and Electronics Engineering, Kadir Has University, 34230, Istanbul, Türkiye
Email: {yizhou,liuxy,pzfan,zma}@swjtu.edu.cn, kezhi.wang@brunel.ac.uk, dongzc666@163.com, eepanay@khas.edu.tr.

***Abstract*—In this paper, a novel artificial noise (AN)-aided secure and covert integrated sensing and communication (ISAC) framework is established for uncrewed aerial vehicle (UAV) systems, to against malicious radar signal detection and communication eavesdropping. Specifically, we consider that besides the communication and sensing signals, the AN signal, which is used to interfere with the eavesdropper and conceal the existence of radar signal, will be transmitted by the UAV-enabled base station (UBS) with uncertainty on its power level. The closed-form expressions of intercept probability (IP) as well as the minimum detection error probability (M-DEP) are derived. Moreover, an efficient communication and sensing performance maximization strategy is designed by optimizing the beamforming vector of communication, covariance matrix of sensing, and UBS receiver filter jointly, to satisfy the IP, power and M-DEP constraints. Simulation results are provided to verify the effectiveness of our joint design by comparing it to benchmark strategy. Moreover, the impact of AN power uncertainty is examined via simulations.**

***Index Terms*—ISAC, UAV, AN uncertainty, covert sensing, secure communication.**

## I. Introduction

Owing to its superiority in enhancing spectrum efficiency and providing additional integration gain, integrated sensing and communication (ISAC) technology has attracted significant attention from both industry and academia [1]. With the capability of integrating communication and sensing functions, ISAC can be well implemented in uncrewed aerial vehicles (UAVs) to support accurate sensing as well as high-quality communication services simultaneously. In [2], an efficient adaptable ISAC design was developed for UAV-empowered system, where the sensing duration can be configured flexibility based on sensing requirements, rather than being the same with the communication period.

However, due to the broadcast nature of wireless communication and the shared spectrum, the security of UAV-ISAC might be compromised [3]–[5]. From the view point of secure communication, to against eavesdropping and protect the legitimate information from being leaked, physical layer security (PLS) technology has been widely adopted in UAV-ISAC system by exploiting the intrinsic channel characteristics. In [6], the real-time secrecy rate was maximized in a UAV-ISAC system where the legitimate user's location was predicted via the extended Kalman filtering and the secrecy rate was maximized by optimizing the UAV trajectory.

Meanwhile, the urgent demand of protecting radar signal from being intercepted has promoted the development of low probability of intercept (LPI) radar. In [7], a LPI design was developed in a multiple-input multiple-output (MIMO) ISAC system to minimize the cyclic frequency sidelobe level, by optimizing the transmitted waveform and precoder of users jointly. In [8], the integrated waveform design was investigated with the aid of reconfigurable intelligent surface, aimed to achieve a LPI by considering the feature of electronic support measure on the radar waveform.

As an efficient solution to further improve security performance, artificial noise (AN) has been considered in ISAC systems. In [9], a secrecy rate maximization algorithm was proposed for ISAC systems with the aid of AN, in the presence of hybrid-colluding eavesdroppers. Moreover, in [10], a dual-function AN supported covert communication design was investigated for ISAC with perfect and imperfect channel state information of the malicious adversary. Although AN has been used in ISAC system to prevent information leakage [9] and enhance the covertness [10] from the communication perspective, to the best of our knowledge, no prior work has considered to employ AN to against malicious radar signal detection and suppress communication eavesdropping simultaneously, thus strongly motivating our work.

To bridge this gap, in this work, a novel AN-aided secure UAV-ISAC framework is proposed to protect the radar signal

This work was supported in part by the National Natural Science Foundation of China under Grant U23A20274, Grant 62361136810, Grant 62301462, Grant 62401483, in part by UKRI Postdoc Guarantee project S-ISAC [grant number EP/Z002435/1] and EU MSCA Postdoctoral Fellowships [grant number 101154926], in part by the Science and Technology Major Project of Tibetan Autonomous Region of China under Grant No.XZ202201ZD0006G04, in part by the Lhasa Science and Technology Plan Project under Grant No. LSKJ202405, in part by the Natural Science Foundation of Sichuan Province under Grants 2025ZNSFSC1446, in part by the Bilateral Scientific Cooperation Program with the China National Science Foundation (NSF), China, and the Scientific and Technical Research Council of Türkiye (TUBITAK), Türkiye under Grant 123N805.

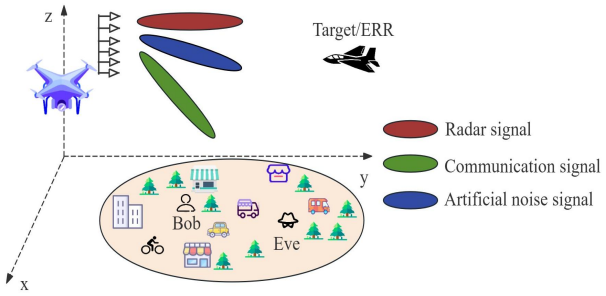


Fig. 1. AN-aided secure and covert UAV-ISAC system.

from being maliciously detected and communication signal from being eavesdropped, by utilizing the uncertainty of AN power. Specifically, a communication and sensing performance maximization problem is formulated by optimizing the beamforming vector of communication, covariance matrix of sensing, and UAV-enabled base station (UBS) receiver filter jointly. However, realizing such a secure framework in UAV-ISAC is challenging due to the quadratic form of beamforming and the coupling among all variables. To deal with this difficulty, alternative optimization (AO), semi-definite relaxation (SDR), sequential rank-one constraint relaxation are adopted to obtain the sub-optimal solutions. Simulation results verify the effectiveness of our proposed solution and highlight the importance of AN on achieving secure and covert UAV-ISAC system.

*Notations:* For a complex scalar $x$, $|x|$ denotes its absolute value. For a vector $\boldsymbol{y}$, $||\boldsymbol{y}||$ and $\boldsymbol{y}^{\boldsymbol{H}}$ represent its Euclidean norm and Hermitian transpose. For a matrix $\boldsymbol{Z}$, Rank($\boldsymbol{Z}$), $\boldsymbol{Z}_{i,j}$ and Tr($\boldsymbol{Z}$) denote its rank, $(i,j)th$ element and trace, respectively.

## II. System Model

### A. Adversary Model

As shown in Fig, 1, we develop a novel AN-aided secure UAV-ISAC system, consisting of one $N$-antenna multi-functional base station that is capable of sending communication, AN and sensing signal simultaneously, one ground communication user Bob, an electronic reconnaissance receiver (ERR) equipped on one target and one eavesdropper (Eve). Consider that the base station is carried by the UAV to provide seamless communication and high-quality sensing services [3], [6]. Let the projection of UBS on the ground as the origin, i.e., $\boldsymbol{r}_u = (0,0)^T$. Denote the horizontal location of target, Bob and Eve as $\boldsymbol{r}_t = (x_t, y_t)^T$, $\boldsymbol{r}_b = (x_b, y_b)^T$, and $\boldsymbol{r}_e = (x_e, y_e)^T$, respectively. The altitudes of UBS and target are defined as $H$ and $H_t$, respectively.

*1) Communication Eavesdropping:* From the communication point of view, since Eve eavesdrops the legitimate transmission between the UBS and Bob, resulting in information leakage. To improve the security performance, AN is transmitted from the UBS to interfere with Eve.

We consider that the UBS sends the AN signal with randomness on its power level. Specifically, assume that the AN signal is independent of both communication and radar signals. Moreover, we consider that the random power for sending AN signal $p_{AN}$ obeys uniform distribution within the range of $[p_{min}, p_{max}]$. Thus, the corresponding probability density function (PDF) is given by

$$f_P(p_{AN}) = \frac{1}{p_{max} - p_{min}}, \forall p_{AN} \in [p_{min}, p_{max}]. \quad (1)$$

*2) Malicious Radar Signal Detection:* From the radar sensing perspective, consider a challenging monitoring scenario where one adversary ERR aims to detect whether the radar signal is being transmitted to sense the surrounding environment. If the ERR detects that the radar signal is not transmitted, it may further launch a more serious attack, i.e., illegal intrusion. Thus, from UBS's point of view, it is expected that the radar signal can be hidden under a certain level of uncertainty to achieve the covertness, so that the ongoing illegal intrusion attack launched by the ERR can be captured. Therefore, it can be observed that the randomness of AN is beneficial to enhance the covertness of the radar signal as well.

Denote $u \in \{1, \cdots, U\}$ as the index of the signal symbol. Let $s_c(u)$, $s_r(u)$, and $s_j(u)$ represent the $u$-th symbol of communication, radar and AN signals, respectively, which are assumed to be independent with zero mean and unit power. Due to the power randomness of the AN signal, the ERR might be confused when detecting whether the radar signal $s_r(u)$, is being transmitted. Let $\mathcal{H}_0$ denote the null hypothesis showing that the radar signal is not transmitted at the UBS, while the alternative hypothesis $\mathcal{H}_1$ shows that the radar signal is transmitted from the UBS to the target/ERR. Thus, from ERR's view, the signal transmitted at the UBS is characterized as

$$\boldsymbol{s}(u) = \begin{cases} \boldsymbol{w}_c s_c(u) + \sqrt{p_{AN}}\boldsymbol{x}_1 s_j(u), & \mathcal{H}_0 \\ \boldsymbol{w}_c s_c(u) + \boldsymbol{w}_r s_r(u) + \sqrt{p_{AN}}\boldsymbol{x}_1 s_j(u). & \mathcal{H}_1 \end{cases} \quad (2)$$

In Eq. (2), $\boldsymbol{w}_c \in \mathbb{C}^{N\times 1}$ is the beamforming vector for the information-bearing signal. Moreover, $\boldsymbol{w}_r \in \mathbb{C}^{N\times 1}$ is the vector for radar signal with

$$\boldsymbol{w}_r \sim \mathcal{CN}(\boldsymbol{0}, \boldsymbol{W}_r), \quad (3)$$

where $\boldsymbol{W}_r \succeq 0$ denotes the covariance matrix of $\boldsymbol{w}_r$. In addition, $\sqrt{p_{AN}}\boldsymbol{x}_1 s_j(u)$ depicts the AN signal with $||\boldsymbol{x}_1||^2 = 1$ and $\boldsymbol{X}_1$ is the covariance matrix of $\boldsymbol{x}$.

### B. Communication Model

Denote $\boldsymbol{h}_q \in \mathbb{C}^{N\times 1}$ as the channel between UBS and device $q, \forall q \in \{b, e\}$, where the subscripts $b$ and $e$ represent Bob and Eve, respectively. Owing to the characteristics of UAV line-of-sight (LoS) propagation, the corresponding channel is model as [3]

$$\boldsymbol{h}_q = \sqrt{\frac{\omega}{d_q^2}}\boldsymbol{a}_q \quad (4)$$

where $\omega$ is the fading coefficient at unit reference distance, $d_q = \sqrt{||\boldsymbol{r}_u - \boldsymbol{r}_q||^2 + H^2}$ depicts the corresponding distance,

and $\boldsymbol{a}_q$ is the steering vector and can be expressed as [3]

$$\boldsymbol{a}_q(\theta_q) = [1, e^{j\frac{2\pi d}{\lambda}\cos\theta_q}, \cdots, e^{j\frac{2(N-1)\pi d}{\lambda}\cos\theta_q}]^T, \quad (5)$$

where $\theta_q$ is the steering angle of the $q$-th device, i.e., $\theta_q = \arccos\left(\frac{H}{d_q}\right)$, $\lambda$ represents the wavelength and $d$ is the distance between adjacent antennas. By doing so, under $\mathcal{H}_1$, the signal received at the Bob is given by

$$y_b(u) = \boldsymbol{h}_b^{\boldsymbol{H}}[\boldsymbol{w}_c s_c(u) + \boldsymbol{w}_r s_r(u) + \sqrt{p_{AN}}\boldsymbol{x}_1 s_j(u)] + n_b(u), \quad (6)$$

where $n_b(u) \sim \mathcal{CN}(0, \sigma_b^2)$ represents the noise at Bob. Thus, Bob's signal-to-interference-plus-noise ratio (SINR) can be expressed as

$$\gamma_b = \frac{\boldsymbol{h}_b^{\boldsymbol{H}}\boldsymbol{W}_c\boldsymbol{h}_b}{\text{Tr}(\boldsymbol{W}_r\boldsymbol{H}_b) + p_{AN}\text{Tr}(\boldsymbol{X}_1\boldsymbol{H}_b) + \sigma_b^2} = \frac{\mathcal{I}_1}{\mathcal{I}_2 + p_{AN}\beta_0}, \quad (7)$$

where $\mathcal{I}_1 = \boldsymbol{h}_b^{\boldsymbol{H}}\boldsymbol{W}_c\boldsymbol{h}_b$, $\mathcal{I}_2 = \text{Tr}(\boldsymbol{W}_r\boldsymbol{H}_b) + \sigma_b^2$, $\beta_0 = \text{Tr}(\boldsymbol{X}_1\boldsymbol{H}_b)$ with $\boldsymbol{W}_c = \boldsymbol{w}_c\boldsymbol{w}_c^{\boldsymbol{H}}$ and $\boldsymbol{H}_b = \boldsymbol{h}_b\boldsymbol{h}_b^{\boldsymbol{H}}$.

Due to the randomness of AN, we consider to apply the average SINR as the reliability measurement, which is given by

$$\begin{aligned}\bar{\gamma}_b &= \mathbb{E}[\gamma_b(p_{AN})] = \frac{1}{p_{max} - p_{min}}\int \frac{\mathcal{I}_1}{\mathcal{I}_2 + p_{AN}\beta_0}dp_{AN} \\ &= \frac{\mathcal{I}_1}{\beta_0(p_{max} - p_{min})}\ln\left(\frac{\mathcal{I}_2 + p_{max}\beta_0}{\mathcal{I}_2 + p_{min}\beta_0}\right).\end{aligned} \quad (8)$$

Similarly, we observe that the signal received at Eve is given by

$$y_e(u) = \boldsymbol{h}_e^{\boldsymbol{H}}[\boldsymbol{w}_c\boldsymbol{s}_c(u) + \boldsymbol{w}_r\boldsymbol{s}_r(u) + \sqrt{p_{AN}}\boldsymbol{x}_1 s_j(u)] + n_e(u), \quad (9)$$

where $n_e(u) \sim \mathcal{CN}(0, \sigma_e^2)$ is the noise at Eve. As such, the Eve's SINR can be formulated as

$$\gamma_e = \frac{\boldsymbol{h}_e^{\boldsymbol{H}}\boldsymbol{W}_c\boldsymbol{h}_e}{\text{Tr}(\boldsymbol{W}_r\boldsymbol{H}_e) + p_{AN}\text{Tr}(\boldsymbol{X}_1\boldsymbol{H}_e) + \sigma_e^2} = \frac{\mathcal{I}_3}{\mathcal{I}_4 + p_{AN}\kappa}, \quad (10)$$

where $\mathcal{I}_3 = \boldsymbol{h}_e^{\boldsymbol{H}}\boldsymbol{W}_c\boldsymbol{h}_e$, $\kappa = \text{Tr}(\boldsymbol{X}_1\boldsymbol{H}_e)$, $\mathcal{I}_4 = \text{Tr}(\boldsymbol{W}_r\boldsymbol{H}_e) + \sigma_e^2$ with $\boldsymbol{H}_e = \boldsymbol{h}_e\boldsymbol{h}_e^{\boldsymbol{H}}$.

Next, we evaluate the secrecy performance by discussing the intercept probability (IP), which implies the occurrence of the event that the SINR of Eve is no less than a pre-defined threshold $\gamma_1$, and is given by

$$\begin{aligned}P_{IP} &= \Pr\left(\frac{\mathcal{I}_3}{\mathcal{I}_4 + p_{AN}\kappa} \geq \gamma_1\right) = \Pr\left(p_{AN} \leq \frac{\mathcal{I}_3 - \mathcal{I}_4\gamma_1}{\kappa\gamma_1}\right) \\ &= \begin{cases} 1, & \mathcal{I}_3 \geq p_{max}\gamma_1\kappa + \gamma_1\mathcal{I}_4 \\ \Omega, & p_{min}\gamma_1\kappa + \gamma_1\mathcal{I}_4 < \mathcal{I}_3 \leq p_{max}\gamma_1\kappa + \gamma_1\mathcal{I}_4 \\ 0, & \mathcal{I}_3 \leq p_{min}\gamma_1\kappa + \gamma_1\mathcal{I}_4, \end{cases}\end{aligned} \quad (11)$$

where $\Pr(\cdot)$ represents the occurrence probability of the corresponding event and

$$\Omega = \int_{p_{min}}^{\frac{\mathcal{I}_3 - \gamma_1\mathcal{I}_4}{\gamma_1\kappa}} \frac{1}{p_{max} - p_{min}}dp_{AN} = \frac{\mathcal{I}_3 - \gamma_1\mathcal{I}_4 - p_{min}\gamma_1\kappa}{\gamma_1\kappa(p_{max} - p_{min})}. \quad (12)$$

In this work, we focus on the scenario when $p_{min}\gamma_1\kappa + \gamma_1\mathcal{I}_4 < \mathcal{I}_3$ and $P_{IP} = \Omega$.

### C. Radar Sensing Model

Let $\theta_t$ as the steering angle of the target/ERR, i.e., $\theta_t = \arccos\left(\frac{|H - H_t|}{d_t}\right)$ with $d_t = \sqrt{(H - H_t)^2 + ||\boldsymbol{r}_u - \boldsymbol{r}_t||^2}$. Thus, the corresponding steering vector can be expressed as [3]

$$\boldsymbol{a}_t(\theta_t) = [1, e^{j\frac{2\pi d}{\lambda}\cos\theta_t}, \cdots, e^{j\frac{2(N-1)\pi d}{\lambda}\cos\theta_t}]^T. \quad (13)$$

*1) Radar Sensing Quality:* As the sensing, communication and AN signals are all emitted from the UBS, after reflecting from the target, the interference of communication and jamming signal can be perfectly eliminated at the UBS. To this end, the received signal at the UBS can be expressed as

$$y_r(u) = \mu^2\boldsymbol{a}_t(\theta_t)\boldsymbol{a}_t^H(\theta_t)\boldsymbol{w}_r s_r(u) + n(u), \quad (14)$$

where $n(u) \sim \mathcal{CN}(0, \sigma^2)$ is the noise at the UBS and $\mu$ depicts the UAV-target/ERR path loss, i.e., $\mu = \sqrt{1/d_t^2}$.

To enhance the radar detection performance, a receiver filter $\boldsymbol{v}$ is adopted to process the received echo signal, yielding the following radar SNR

$$\gamma_r = \frac{\mu^4\boldsymbol{v}^H\boldsymbol{A}(\theta_t)\boldsymbol{W}_r\boldsymbol{A}^H(\theta_t)\boldsymbol{v}}{\sigma^2\boldsymbol{v}^H\boldsymbol{v}}, \quad (15)$$

where $\boldsymbol{A}(\theta_t) = \boldsymbol{a}_t(\theta_t)\boldsymbol{a}_t(\theta_t)^{\boldsymbol{H}}$.

*2) Malicious Detection:* According to the introduced model, it can be seen that the hypothesis at the target/ERR for the $u$-th symbol is given by [11]

$$y_t(u) = \begin{cases} \mu\boldsymbol{a}_t^H(\theta_t)[\boldsymbol{w}_c s_c(u) + \sqrt{p_{AN}}\boldsymbol{x}_1 s_j(u)] + n_t(u), & \mathcal{H}_0 \\ \mu\boldsymbol{a}_t^H(\theta_t)[\boldsymbol{w}_c s_c(u) + \boldsymbol{w}_r s_r(u) + \sqrt{p_{AN}}\boldsymbol{x}_1 s_j(u)] + n_t(u), & \mathcal{H}_1, \end{cases} \quad (16)$$

where $n_t(u) \sim \mathcal{CN}(0, \sigma_t^2)$ is the noise at the target/ERR.

Inspired by [10], the average power received in the ERR. i.e., $\xi = \frac{1}{U}\sum_{u=1}^{U}|y_t(u)|^2$, is adopted to further compare with the detection threshold $\tau$, and the corresponding decision rule can be expressed as

$$\xi \underset{\mathcal{D}_0}{\overset{\mathcal{D}_1}{\gtrless}} \tau, \quad (17)$$

where $\mathcal{D}_0$ and $\mathcal{D}_1$ are the corresponding decisions in favor of $\mathcal{H}_0$ and $\mathcal{H}_1$, respectively. In the case of infinite blocklength, based on the strong law of large numbers, the average power $\xi$ can be rewritten as

$$\xi = \begin{cases} \mathcal{W}_1 + \mu^2 p_{AN}\text{Tr}(\boldsymbol{X}_1\boldsymbol{A}(\theta_t)), & \mathcal{H}_0 \\ \mathcal{W}_1 + \mu^2\text{Tr}(\boldsymbol{W}_r\boldsymbol{A}(\theta_t)) + \mu^2 p_{AN}\text{Tr}(\boldsymbol{X}_1\boldsymbol{A}(\theta_t)), & \mathcal{H}_1, \end{cases} \quad (18)$$

where $\mathcal{W}_1 = \mu^2\boldsymbol{a}_t^H(\theta_t)\boldsymbol{W}_c\boldsymbol{a}_t(\theta_t) + \sigma_t^2$.

*3) Detection Analysis at ERR:* To further investigate the detection performance in the ERR, it is important to discuss the statistical distribution of $\xi$ under different hypotheses. We note that the randomness of $\xi$ comes from the uncertainty of AN power, which is assumed to obey uniform distribution as introduced in Eq. (1).

Next, detection performance is investigated by analyzing two types of detection error, i.e., false alarm probability (FAP) and miss detection probability (MDP). The FAP, which implies that the ERR mistakenly judges that the radar signal

is transmitted from the UBS when $\mathcal{H}_0$ occurs, and can be expressed as

$$P_{FA} = \Pr(\mathcal{D}_1|\mathcal{H}_0) = \Pr(p_{AN}\beta_1 + \mathcal{W}_1 \geq \tau) = \begin{cases} 1, & \tau \leq p_{min}\beta_1 + \mathcal{W}_1 \\ \Gamma_1, & p_{min}\beta_1 + \mathcal{W}_1 < \tau \leq p_{max}\beta_1 + \mathcal{W}_1. \\ 0, & \tau \geq p_{max}\beta_1 + \mathcal{W}_1. \end{cases} \tag{19}$$

where $\beta_1 = \mu^2 \mathrm{Tr}(\boldsymbol{X}_1 \boldsymbol{A}(\theta_t))$, and

$$\Gamma_1 = \int_{\frac{\tau-\mathcal{W}_1}{\beta_1}}^{p_{max}} \frac{1}{p_{max} - p_{min}} dp_{AN} = \frac{p_{max}\beta_1 - \tau + \mathcal{W}_1}{p_{max}\beta_1 - p_{min}\beta_1}. \tag{20}$$

In addition, the MDP, which depicts the probability that the ERR falsely misses the radar signal when $\mathcal{H}_1$ happens, and can be expressed as

$$P_{MD} = \Pr(\mathcal{D}_0|\mathcal{H}_1) = \Pr(p_{AN}\beta_1 + \mathcal{W}_2 \leq \tau) = \begin{cases} 1, & \tau \geq p_{max}\beta_1 + \mathcal{W}_2 \\ \Gamma_2, & p_{min}\beta_1 + \mathcal{W}_2 < \tau \leq p_{max}\beta_1 + \mathcal{W}_2 \\ 0, & \tau < p_{min}\beta_1 + \mathcal{W}_2. \end{cases} \tag{21}$$

where $\mathcal{W}_2 = \mu^2 \boldsymbol{a}_t^H(\theta_t)\boldsymbol{W}_c\boldsymbol{a}_t(\theta_t) + \mu^2 \mathrm{Tr}(\boldsymbol{W}_r \boldsymbol{A}(\theta_t)) + \sigma_t^2$, and

$$\Gamma_2 = \int_{p_{min}}^{\frac{\tau-\mathcal{W}_2}{\beta_1}} \frac{1}{p_{max} - p_{min}} dp_{AN} = \frac{\tau - \mathcal{W}_2 - p_{min}\beta_1}{p_{max}\beta_1 - p_{min}\beta_1}. \tag{22}$$

Following [12], we assume that the prior probabilities of $\mathcal{H}_0$ and $\mathcal{H}_1$ to be equal and employ the detection error probability (DEP) as the radar signal detection indicator, i.e., $P_E = P_{FA} + P_{MD}$. Next, the minimum DEP of warden is studied in the following Lemma.

**Lemma 1.** *The minimum DEP of warden is given by*

$$P_{E,min} = 1 - \frac{\mu^2 Tr(\boldsymbol{W}_r \boldsymbol{A}(\theta_t))}{p_{max}\beta_1 - p_{min}\beta_1} \tag{23}$$

***Proof***. By adding $P_{FA}$ and $P_{MD}$ and focusing on the scenario when $p_{min}\beta_1 + \mathcal{W}_2 \leq p_{max}\beta_1 + \mathcal{W}_1$, we have

$$P_E = P_{FA} + P_{MD} = \begin{cases} 1, & \tau \geq p_{max}\beta_1 + \mathcal{W}_2 \\ \Gamma_2, & p_{max}\beta_1 + \mathcal{W}_1 \leq \tau \leq p_{max}\beta_1 + \mathcal{W}_2 \\ \Gamma_1 + \Gamma_2, & p_{min}\beta_1 + \mathcal{W}_2 \leq \tau \leq p_{max}\beta_1 + \mathcal{W}_1 \\ \Gamma_1, & p_{min}\beta_1 + \mathcal{W}_1 \leq p_{min}\beta_1 + \mathcal{W}_2 \\ 1, & \tau < p_{min}\beta_1 + \mathcal{W}_1. \end{cases} \tag{24}$$

According to Eqs (20) and (22), We observe that with increasing $\tau$, $\Gamma_1$ monotonically decreases while $\Gamma_2$ monotonically increases. In addition, as $\Gamma_1 + \Gamma_2 = 1 - \frac{\mu^2 \mathrm{Tr}(\boldsymbol{W}_r \boldsymbol{A}(\theta_t))}{p_{max}\beta_1 - p_{min}\beta_1}$, which is independent of $\tau$. Therefore, according to the monotonicity of $P_E$ in terms of $\tau$, we can observe that the minimum DEP is shown as Eq. (23). □

### *D. Problem Formulation*

In this work, we formulate a communication and sensing performance maximization problem by designing the beamforming vector of communication, covariance matrix of sensing, and UBS receiver filter jointly, while satisfying special requirements of radar signal covertness, power budget and communication security. As such, the optimization problem can be formulated as

$$\underset{\boldsymbol{v}, \boldsymbol{w}_c, \boldsymbol{W}_r}{\text{maximize}} \ \gamma_r + \bar{\gamma}_b \tag{25a}$$

$$\text{s.t. } \mathrm{Tr}(\boldsymbol{W}_r) + ||\boldsymbol{w}_c||^2 + p_{max} \leq P_0 \tag{25b}$$

$$0 \leq P_{IP} \leq \delta_1 \tag{25c}$$

$$P_{E,min} \geq \delta_2 \tag{25d}$$

where constraint (25b) is the maximum power constraint at the UBS, constraint (25c) specifies that the IP of Eve should be no greater than a given threshold $\delta_1$, constraint (25d) requires that the minimum DEP at the ERR should be no less than the threshold $\delta_2$. Due to the the quadratic form of the beamforming and coupling effect among all variables, we note that Problem (25) is challenging to solve.

## III. Proposed Solution

In this section, an efficient communication and sensing performance maximization solution is proposed by adopting a series of mathematical solutions.

First, based on the matrix transformation, we have

$$\boldsymbol{h}_b^{\boldsymbol{H}} \boldsymbol{W}_c \boldsymbol{h}_b = \mathrm{Tr}(\boldsymbol{h}_b^{\boldsymbol{H}} \boldsymbol{W}_c \boldsymbol{h}_b) = \mathrm{Tr}(\boldsymbol{W}_c \boldsymbol{h}_b \boldsymbol{h}_b^{\boldsymbol{H}}) = \mathrm{Tr}(\boldsymbol{W}_c \boldsymbol{H}_b). \tag{26}$$

After a series of similar mathematical manipulations, we observe that the IP constraint of (25c) can be re-expressed as

$$\begin{aligned} &\mathrm{Tr}(\boldsymbol{W}_c \boldsymbol{H}_e) - \gamma_1 \mathrm{Tr}(\boldsymbol{W}_r \boldsymbol{H}_e) - \gamma_1 \sigma_e^2 \leq c_1 \gamma_1 \mathrm{Tr}(\boldsymbol{X}_1 \boldsymbol{H}_e), \\ &\mathrm{Tr}(\boldsymbol{W}_c \boldsymbol{H}_e) - \gamma_1 (\mathrm{Tr}(\boldsymbol{W}_r \boldsymbol{H}_e) + \sigma_e^2) - p_{min}\gamma_1 \mathrm{Tr}(\boldsymbol{X}_1 \boldsymbol{H}_e) \geq 0, \end{aligned} \tag{27}$$

where $c_1 = \delta_1(p_{max} - p_{min}) + p_{min}$. In addition, the minimum DEP constraint of (25d) is re-formulated as

$$c_2 \mathrm{Tr}(\boldsymbol{X}_1 \boldsymbol{A}(\theta)) \geq \mathrm{Tr}(\boldsymbol{W}_r \boldsymbol{A}(\theta)), \tag{28}$$

where $c_2 = (1 - \delta_2)(p_{max} - p_{min})$.

With above transformation, by introducing two slack variables $\chi$ and $\iota$, the original problem (25) can be transformed as

$$\underset{\boldsymbol{v}, \boldsymbol{W}_c, \boldsymbol{W}_r, \chi, \iota}{\text{maximize}} \ \frac{\mu^4 \boldsymbol{v}^H \boldsymbol{A}(\theta_t) \boldsymbol{W}_r \boldsymbol{A}^H(\theta_t) \boldsymbol{v}}{\sigma^2 \boldsymbol{v}^H \boldsymbol{v}} + \underbrace{\frac{1}{\chi c_3} \ln\left(1 + \frac{c_3}{\iota + c_4}\right)}_{\mathcal{W}}. \tag{29a}$$

$$\text{s.t. } \mathrm{Tr}(\boldsymbol{W}_r) + \mathrm{Tr}(\boldsymbol{W}_c) + p_{max} \leq P_0 \tag{29b}$$

$$\mathrm{Rank}(\boldsymbol{W}_c) = 1, \boldsymbol{W}_r \succeq 0, \tag{29c}$$

$$\frac{1}{\chi} \leq \mathrm{Tr}(\boldsymbol{W}_c \boldsymbol{H}_b) \tag{29d}$$

$$\iota \geq \mathrm{Tr}(\boldsymbol{W}_r \boldsymbol{H}_b) \tag{29e}$$

$$(27),\ (28),$$

where $c_3 = \beta_0(p_{max} - p_{min})$ and $c_4 = \sigma_b^2 + p_{min}\beta_0$. We remark that the constraint $\mathrm{Rank}(\boldsymbol{W}_c) = 1$ needs to be satisfied to transmit the communication signal. Next, we employ AO method to decouple the original optimization problem into two sub-problems to solve $\{\boldsymbol{w}_c, \boldsymbol{W}_r\}$ and $\boldsymbol{v}$ in an iterative manner.

### A. Solve $\boldsymbol{W}_c$ and $\boldsymbol{W}_r$

By fixing $\boldsymbol{v}$, we first address the optimization of $\{\boldsymbol{W}_c, \boldsymbol{W}_r\}$. To proceed, it is known that $\frac{1}{x}\ln\left(1+\frac{1}{y}\right)$ is jointly convex in terms of $x$ and $y$ [13]. Next, to make the objective function in Eq. (29a) concave, the first-order Taylor expansion is adopted to approximate $\mathcal{W}$ as $\mathcal{W}_1$, which is given by

$$\mathcal{W}_1 = \frac{1}{\chi^{(l)}c_3}\ln\left(1+\frac{c_3}{\iota^{(l)}+c_4}\right) - \frac{\chi-\chi^{(l)}}{(\chi^{(l)})^2 c_3}\ln\left(1+\frac{c_3}{\iota^{(l)}+c_4}\right) - \frac{(\iota-\iota^{(l)})}{\chi^{(l)}[(\iota^{(l)}+c_4)^2+(\iota^{(l)}+c_4)c_3]}, \tag{30}$$

Moreover, $\chi^{(l)}$ and $\iota^{(l)}$ are the values of $\chi$ and $\iota$ in the $l$-th iteration in the outer loop, respectively. Although the objective function is approximated, another difficulty in solving Problem (29) is the rank-one constraint. Note that for a rank-one matrix, the trace of the matrix equals to its largest eigenvalue. Next, inspired by [14], we consider to relax the rank-one constraint $\text{Rank}(\boldsymbol{W}_c) = 1$ by replacing it with its relaxed convex constraint which quantifies the ratio of its largest eigenvalue to the trace of $\boldsymbol{W}_c$ through a factor $\varrho \in [0,1]$. By doing so, $\boldsymbol{W}_c$ and $\boldsymbol{W}_r$ can be obtained by solving

$$\underset{\boldsymbol{W}_c,\boldsymbol{W}_r,\chi,\iota}{\text{maximize}} \ \frac{\mu^4 \boldsymbol{v}^H \boldsymbol{A}(\theta_t)\boldsymbol{W}_r\boldsymbol{A}^H(\theta_t)\boldsymbol{v}}{\sigma^2\boldsymbol{v}^H\boldsymbol{v}} + \mathcal{W}_1 \tag{31a}$$

$$\text{s.t. } \boldsymbol{W}_r \succeq 0 \tag{31b}$$

$$\boldsymbol{u}_{max}(\boldsymbol{W}_c^{(n)})^H \boldsymbol{W}_c \boldsymbol{u}_{max}(\boldsymbol{W}_c^{(n)}) \geq \varrho^{(n)}\text{Tr}(\boldsymbol{W}_c) \tag{31c}$$

$$(27),\ (28),\ (29b), (29d), (29e),$$

where $\boldsymbol{u}_{max}(\boldsymbol{W}_c)$ is the eigenvector associated with the maximum eigenvalue $\lambda_{max}$ of the matrix $\boldsymbol{W}_c$ and $\boldsymbol{u}_{max}(\boldsymbol{W}_c^n)$ depict the value of $\boldsymbol{u}_{max}(\boldsymbol{W}_c)$ in the $n$-th iteration in the inner loop. Moreover, $\varrho^{(n)}$ is the value of $\varrho$ in the $n$-th iteration in the inner loop. We summarize the solution of solving Problem (31) in Algorithm 1.

**Algorithm 1** Solution for solving Problem (31).

1: Initialize: Set feasible $\boldsymbol{W}_c$, $\chi$, $\iota$ and $n=0$;
2: Set $\varrho^{(n)}=0$, obtain $\boldsymbol{W}_c^{(n)}$ and $\boldsymbol{W}_r^{(n)}$ by solving Problem (31);
3: initial step size $\delta^{(n)} \in \left(0, 1-\frac{\lambda_{max}\left(\boldsymbol{W}_c^{(n)}\right)}{\text{Tr}(\boldsymbol{W}_c^{(n)})}\right)$;
4: **repeat**
5: Based on $\{\boldsymbol{W}_c^{(n)}, \varrho^{(n)}\}$, solve Problem (31).
6: **if** Problem (31) is solvable **then**
7: Obtain $\boldsymbol{W}_c^{(n+1)}$ by solving Problem (31) and update $\delta^{(n+1)}=\delta^{(n)}$;
8: **else**
9: Update $\boldsymbol{W}_c^{(n+1)}=\boldsymbol{W}_c^{(n)}$ and $\delta^{(n+1)}=\delta^{(n)}/2$;
10: **end if**
11: $\varrho^{(n+1)} = \min\left(1, \frac{\lambda_{max}\left(\boldsymbol{W}_c^{(n+1)}\right)}{\text{Tr}(\boldsymbol{W}_c^{(n+1)})}+\delta^{(n+1)}\right)$;
12: $\chi^{(n+1)}=\chi^{(n)}$, $\iota^{(n+1)}=\iota^{(n)}$;
13: $n=n+1$;
14: **until** $|1-\varrho^{(n-1)}| \leq 10^{-3}$.

### B. Solve $\boldsymbol{v}$

Given $\{\boldsymbol{W}_c, \boldsymbol{W}_r\}$, by removing the constant terms in the objective function, the receiver filter can be obtained by solving

$$\underset{\boldsymbol{v}}{\text{maximize}} \ \frac{\mu^4 \boldsymbol{v}^H \boldsymbol{A}(\theta_t)\boldsymbol{W}_r\boldsymbol{A}^H(\theta_t)\boldsymbol{v}}{\sigma^2\boldsymbol{v}^H\boldsymbol{v}}. \tag{32a}$$

It can be seen that Problem (32) is a typical Rayleigh quotient problem [15]. Thus, the optimal $\boldsymbol{v}^*$ is given by

$$\boldsymbol{v}^* = \boldsymbol{V}_{max}((\sigma^2)^{-1}\mu^4 \boldsymbol{A}(\theta_t)\boldsymbol{W}_r\boldsymbol{A}^H(\theta_t)), \tag{33}$$

where $\boldsymbol{V}_{max}(\boldsymbol{X})$ is the eigenvector associated with the maximum eigenvalue of the matrix $\boldsymbol{X}$.

### C. Overall Algorithm

We summarize the detail process for solving Problem (25) in Algorithm 2, where $\{\boldsymbol{W}_c, \boldsymbol{W}_r\}$ and $\boldsymbol{v}$ are solved iteratively. As our proposed Algorithm 2 leads to a non-decreasing sequence of the objective value, thus, the proposed solution is guaranteed to converge.

**Algorithm 2** Proposed Solution for solving Problem (25).

1: Initialize: Set feasible $\boldsymbol{v}^{(0)}$,$\mathbf{W}_c^{(0)}$,$\mathbf{W}_r^{(0)}$, $\chi^{(0)}$,$\iota^{(0)}$; Set $\boldsymbol{x}_1$ to satisfy $||\boldsymbol{x}_1||^2=1$, and $l=1$
2: **repeat**
3: Update $\mathbf{W}_c^{(l)}$ and $\mathbf{W}_r^{(l)}$ via solving Problem (31) and Algorithm 1;
4: Update $\mathbf{v}$ based on (33);
5: $l=l+1$;
6: **until** convergence.

## IV. Simulation Results

In this section, we evaluate the performance of our AN-aided secure UAV-ISAC design using simulations. We consider that the UBS is with 4 antennas and set the locations of target/ERR, Bob, Eve and target at $\boldsymbol{r}_t = (300, 250)^T$, $\boldsymbol{r}_b = (100, 200)^T$, and $\boldsymbol{r}_e = (150, 300)^T$, respectively. The UBS and target are at deployed 100 m and 300 m, respectively. In addition, we set $\omega = 1$, $\sigma_b^2 = \sigma_e^2 = \sigma_t^2 = -90$ dBm, $\sigma^2 = -100$ dBm, $d/\lambda = 0.5$, $\gamma_1 = 1$ dB, $\delta_1 = 0.1$, $\delta_2 = 0.8$, $P_0 = 20$ W, $p_{min} = 0.5$ W and $p_{max} = 2$ W.

In Fig. 2, the objective value versus number of iteration is plotted. It can be seen that our proposed solution converges within 6 iterations, thus verifying the convergence of our design. Moreover, in this simulation, we observe that with a more strict IP constraint, i.e., a lower value of $\delta_1$, a sacrificed objective value is obtained, showing the trade-off between communication security constraint and objective value.

Then, we evaluate the advantages of our proposed Algorithm 2 in improving communication and sensing performance by comparing it with the following benchmark solution.

- "Random Receiver Filter Design" Benchmark Solution: in this scheme, beamforming vector of communication and covariance matrix of sensing are optimized via Algorithm 1, while the receiver filter is fixed with its initial value.

In Fig. 3, we compare our proposed Algorithm 2 to benchmark scheme over a wide range of covert sensing requirement $\delta_2$. First, it can be seen that our proposed Algorithm 2 outperforms benchmark solution among all values of $\delta_2$, thus

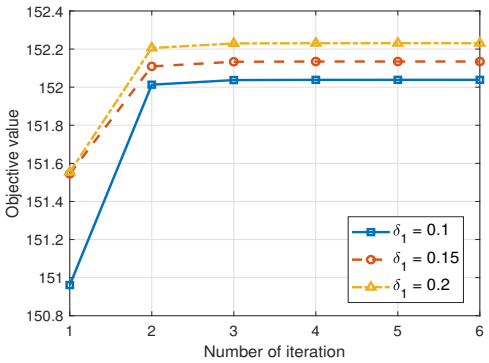


Fig. 2. Objective value versus number of iteration.

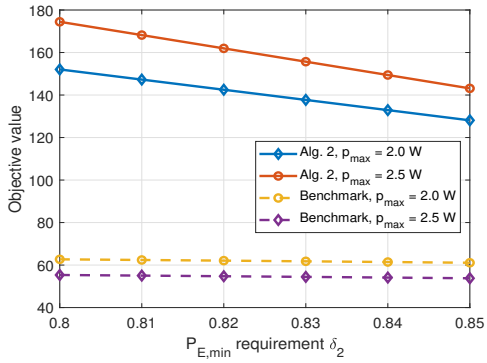


Fig. 3. Objective value versus covert sensing requirement $\delta_2$.

highlighting the benefit of our joint optimizing design. Next, we observe that a higher value of $\delta_2$ leads to a lower objective value. This is because, with a more strict covert sensing requirement and a higher $\delta_2$, to achieve covertness, less power will be assigned to transmit the radar signal according to Eq. (23), and the radar SNR is compromised by the covert sensing constraint. Specifically, for our proposed Alg. 2, when $p_{max} = 2.5$ W and $\delta_2 = 0.8$, 2.69 W is allocated for sending radar signal, contributing to a high radar SNR of 119.95 and an average Bob's SINR of 54.50. While when $\delta_2$ increases to 0.85, 2.42 W is allocated for sending radar signal with a reduced radar SNR of 89.96, and the average Bob's SINR is 53.17.

In addition, as we can see from Fig 3, for our proposed Alg. 2, when $p_{max} = 2.5$ W, the achieved objective value is greater than that of when $p_{max} = 2$ W. This phenomenon is due to the fact that, when $p_{max}$ increases, under the cover of increased AN uncertainty, a higher amount of power is allowed to transmit the radar signal to achieve a better radar SNR. Since the radar SNR is dominant, thus, a higher objective value is achieved. While for the benchmark scheme, the phenomenon is opposite. Without the radar filter design, the radar SNR is much lower than average Bob's SINR. In this condition, with a less AN power, more residual power can be used for sending communication signal and further enhance the objective value.

## V. Conclusion

In this paper, by utilizing the uncertainty of AN power, a AN-aided secure UAV-ISAC was developed to against malicious radar signal detection and communication eavesdropping. In specific, under the AN power uncertainty, the closed-form expressions of IP and M-DEP were investigated theoretically. Moreover, an efficient communication and sensing performance maximization algorithm was designed by optimizing the beamforming vector of communication, covariance matrix of sensing, and UBS receiver filter jointly, subject to certain IP, power and M-DEP requirements. Simulation results verified the effectiveness of our design by comparing it to benchmark scheme and demonstrated the impact of AN power uncertainty.

## References


[1] J. Ye, J. Dai, C. Pan, K. Wang and J. Li, "Joint Active and Passive Beamforming Design for Secure RIS-Aided ISAC System," *in IEEE Wireless Communications Letters,* vol. 14, no. 3, pp. 916-920, March 2025.

[2] C. Deng, X. Fang and X. Wang, "Beamforming Design and Trajectory Optimization for UAV-Empowered Adaptable Integrated Sensing and Communication," in *IEEE Transactions on Wireless Communications,* vol. 22, no. 11, pp. 8512-8526, Nov. 2023.

[3] D. Deng, W. Zhou, X. Li, D. B. Da Costa, D. W. K. Ng, and A. Nallanathan, "Joint Beamforming and UAV Trajectory Optimization for Covert Communications in ISAC Networks," accepted in *IEEE Trans. Wireless Commun.,* 2024, doi: 10.1109/TWC.2024.3503726.

[4] Z. Yang, S. Zhang, G. Chen, Z. Dong, Y. Wu and D. Benevides da Costa, "Secure Integrated Sensing and Communication Systems Assisted by Active RIS," in *IEEE Transactions on Vehicular Technology,* vol. 73, no. 12, pp. 19791-19796, Dec. 2024.

[5] Y. Zhou, P. Fan and Z. Ma, "A UAV-Enabled Integrated Sensing and Covert Communication System," accepted in *IEEE Transactions on Vehicular Technology,* 2025, doi: 10.1109/TVT.2025.3548022.

[6] J. Wu, W. Yuan and L. Hanzo, "When UAVs Meet ISAC: Real-Time Trajectory Design for Secure Communications," in *IEEE Transactions on Vehicular Technology*, vol. 72, no. 12, pp. 16766-16771, Dec. 2023.

[7] Q. Shi, Y. Wang, Z. Zhou, G. Cui and P. Fan, "Low Probability of Intercept Signal Design for MIMO Integrated Sensing and Communication Systems," accepted in *IEEE Transactions on Communications,* 2025.

[8] X. Liu, Y. Yuan, T. Zhang, G. Cui and W. P. Tay, "Integrated Transmit Waveform and RIS Phase Shift Design for LPI Detection and Communication," in *IEEE Transactions on Wireless Communications,* vol. 23, no. 6, pp. 5663-5679, June 2024.

[9] M. Liu et al., "Joint Beamforming Design for Integrated Sensing and Communication Systems with Hybrid-Colluding Eavesdroppers," accepted in *IEEE Transactions on Communications,* 2025, doi: 10.1109/TCOMM.2025.3538835.

[10] R. Tang, L. Yang, L. Lv, Z. Zhang, Y. Liu, and J. Chen, "Dual-Functional Artificial Noise (DFAN) Aided Robust Covert Communications in Integrated Sensing and Communications," accepted in *IEEE Trans. Commun.*,2024, doi: 10.1109/TCOMM.2024.3451619.

[11] Y. Zhang et al., "Robust Transceiver Design for Covert Integrated Sensing and Communications With Imperfect CSI," accepted in *IEEE Transactions on Communications*, 2024 doi: 10.1109/TCOMM.2024.3387869.

[12] C. Wang, Z. Li and D. W. K. Ng, "Covert Rate Optimization of Millimeter Wave Full-Duplex Communications," in *IEEE Transactions on Wireless Communications,* vol. 21, no. 5, pp. 2844-2861, May 2022.

[13] C. Xu, C. Zhan, H. Yang and L. Xiao, "Pareto-Optimal Aerial-Ground Energy Minimization for Aerial 3D Mobile Edge Computing Networks," in *IEEE Transactions on Vehicular Technology,* vol. 73, no. 5, pp. 7218-7233, May 2024.

[14] Z. Liu, X. Li, H. Ji, and H. Zhang, "Active STAR-RIS Enabled ISAC Networks Against Simultaneous Eavesdropping and Detection Attacks," accepted in *IEEE Internet of Things Journal,* 2025, doi: 10.1109/JIOT.2025.3534290.

[15] R. Li, Q. Zhang, D. Ma, K. Yu, and Y. Huang, "Joint Target Assignment and Resource Allocation for Multi-Base Station Cooperative ISAC in UAV Detection," accepted in *IEEE Transactions on Vehicular Technology*, 2025, doi: 10.1109/TVT.2025.3525980.